

Prediction of Wax Pattern Dimensions in Investment Casting

A. S. Sabau and S. Viswanathan
Metals and Ceramics Division
Oak Ridge National Laboratory
Oak Ridge, TN 37831-6083

Copyright 2002 American Foundry Society

ABSTRACT

Dimensional changes between a pattern die and its corresponding investment cast part occur as a result of complex phenomena such as thermal expansion/contraction and hot deformation (elastic, plastic, and creep) during the processing of the pattern material (wax), mold material (shell), and solidifying alloy. In this study, wax pattern dimensions are determined using computer models that take into account the thermophysical and rheological behavior of the wax. Pattern dimensions are calculated using a three-dimensional finite element model for coupled thermal and mechanical analysis developed within the commercial software ABAQUS™. Cerita™ 29-51, an industrial wax is considered in this study. The effects of restraint geometrical features by the metal die, and process parameters such as dwell time, die/platen temperature, injection pressure and injection temperature are also considered. The results of numerical simulation are compared with experimental measurements on test patterns. Measurements of the temperature at the injection port, pressure in the die cavity, and the results of numerical simulations provide several insights into the wax injection process. Viscoelastic models exhibit good potential for accurately capturing the details of wax pattern deformation. Conversely, pure elastic models are unsuitable for predicting deformation, as any distortion is completely relaxed once the pattern is removed from the die.

INTRODUCTION

The investment casting process consists of making a disposable wax pattern by injecting wax into a metal mold, building a ceramic shell mold around the wax pattern by the application of a series of ceramic coatings to the wax pattern, dewaxing the ceramic shell mold, and casting the alloy into the shell mold. Dimensional changes between the pattern tooling and its corresponding cast part occur as a result of thermal expansion, shrinkage, hot deformation, and creep of the pattern material (wax), mold material (shell), and solidifying alloy during the processing (Piwonka and Wiest, 1998).

The difference between the die dimensions and corresponding casting dimensions are usually referred to as the tooling allowances for the pattern die. Tooling allowances are estimated from the part dimensions based on dimensional changes associated with the wax, shell, and alloy systems. Recent surveys conducted by the Investment Casting Institute on dimensioning practices used in the investment casting industry found that die dimensions are reworked by trial-and-error procedures until casting dimensions are produced within acceptable dimensional tolerances, increasing the lead time and cost of the manufacturing process (Okhuysen et al., 1998).

Wax pattern deformation has a large effect on tooling allowances. Rosenthal (1979) and Okhuysen et al. (1998) indicated that the shrinkage of the wax is one of the largest components of the overall dimensional change between the pattern tooling and its corresponding cast part. Control of the wax pattern dimensions is thus a critical step in the investment casting process. In order to predict the pattern tooling allowances, all the factors that determine dimensional changes associated with wax processing must be evaluated.

The use of computer models for the prediction of wax dimensions has been hindered by the lack of data for constitutive equations of thermomechanical behavior. The evaluation of the thermomechanical characteristics of waxes used in the investment casting industry is based on engineering behavior (Horacek and Helan, 1998; Fielder, 1998; and BICTA 1983, 1985), such as cavitation propensity and volumetric expansion, rather than by the local deformation of the wax determined by physical and computational models (Chakravorty, 1999). Recently, Sabau and Viswanathan (2000), documented experimental measurements on CERITA™ 29-51, an industrial, unfilled wax, with data on material properties that can be used for numerical simulations. These properties are used in this study and are briefly presented in the next section. The wax pattern dimensions are determined using a three-dimensional finite element model for coupled thermal and mechanical analysis developed within ABAQUS™. The following factors are considered in the analysis: the restraint due to geometrical features in the metal die, and process parameters such as dwell time, die/platen temperature, injection pressure and injection temperature. Numerical simulation results for the wax pattern dimensions are presented and discussed.

THERMOPHYSICAL PROPERTIES OF CERITA™ 29-51 WAX

In this section, experimental data on thermophysical and thermomechanical properties are presented for an unfilled wax, Cerita™ 29-51 (provided by M. Argueso & Co, Inc). Since this wax is currently used in industry, and is a complex blend of polymers (paraffin wax-70% carbon chain length C25-C30, microcrystalline wax, a polymer, and synthetic hydrocarbon resin), its study is of both industrial and scientific importance. The following specifications were supplied by the manufacturer: ring and ball softening point (80-83°C); drop melt point (86-92°C); thermal diffusivity (11.40e-8 m²/s); latent heat (70-90 J/g); density at 25°C (0.968-0.988 g/cm³); and density at 110°C (0.846 g/cm³). The density as a function of temperature was obtained from thermomechanical analysis (TMA) (Sabau and Viswanathan, 2000).

Data on thermal conductivity and specific heat are shown in Table 1. Thermal conductivity was measured using a transient line-source technique, following ASTM standard D 5930-97. During this work, it became apparent that the hot disk technique (Gustafsson, 1991), is not appropriate for this material since, due to the large amount of thermal expansion, it pulls away from the sensor plate. The poor contact between the sensor plate and material results in lower values for thermal conductivity being measured in the solid state than in the liquid state, contrary to the data reported in the literature (Roux et al., 1974). Accordingly, previously reported data obtained using the hot disk technique (Sabau and Viswanathan, 2000) is not accurate. Also, the measured values of specific heat reported are consistent with other data on waxes (Himran et al., 1994), and are more accurate than previously reported values for Cerita™ 29-51 (Sabau and Viswanathan, 2000).

Table 1. Thermophysical properties of Cerita™ 29-51 wax.

Temperature (°C)	Specific Heat (J/gK)	Temperature (°C)	Specific Heat (J/gK)	Temperature (°C)	Thermal Conductivity (W/mK)
25.00	2.2925	49.10	6.0096	21.0	0.211*
30.00	2.6742	53.91	3.0489	56.0	0.211
35.00	3.3337	55.50	2.7384	62.0	0.193
45.00	6.0332	60.00	2.5429	67.0	0.158
47.50	6.3725	80.00	2.2677	97.0	0.154

*Thermal conductivity is assumed to be constant at low temperatures, since, due to the wax shrinkage, there is a poor contact between the sensor and wax that yields an unrealistic low thermal conductivity.

CONSTITUTIVE EQUATIONS FOR MODELING WAX DEFORMATION

Waxes exhibit linear viscoelastic behavior. Viscoelastic materials exhibit relaxation, creep, and dissipative characteristics. For materials that exhibit linear viscoelastic behavior, computer models for the numerical simulation of stress, strain, and the ensuing displacement fields have been developed (Taylor et al., 1970; Zocher et al., 1997; Kaliske and Rothert, 1997; and Poon and Ahmad, 1998). By neglecting inertial effects, the momentum equation is given by Cauchy's second law of motion:

$$\nabla\sigma + \rho\mathbf{g} = 0, \tag{Equation 1}$$

where \mathbf{g} is the gravity vector. The components of the strain tensor are given as a function of displacements (u_1, u_2, u_3), as $\epsilon_{ij} = (\partial u_i / \partial x_j + \partial u_j / \partial x_i) / 2$. In order to illustrate the constitutive equations for waxes, it is convenient to introduce the deviatoric stress tensor, $\mathbf{s} = \sigma - \mathbf{I}\sigma_0/3$, and deviatoric strain tensor, $\mathbf{e} = \epsilon - \mathbf{I}\epsilon_0/3$. The $\sigma_0 = \text{tr } \sigma$ and $\epsilon_0 = \text{tr } \epsilon$ are the hydrostatic stress and dilatation components of the stress and strain tensors, respectively.

SHEAR MODULUS

If the wax is assumed to be an isotropic material, the viscoelastic constitutive equation for the deviatoric stress and strain tensors is given by:

$$\mathbf{s} = 2 \int_0^t G(t - \tau, T) \dot{\mathbf{e}} d\tau, \tag{Equation 2}$$

where G is the shear relaxation modulus (Ferry, 1980). The shear modulus was determined from dynamical mechanical analysis (DMA) measurements (Sabau and Viswanathan, 2000). Shear oscillatory measurements were carried out at temperatures of 25 to 55°C at 5°C increments using a Rheometric Scientific Advanced Rheometric Expansion System (ARES). The material was tested on a torsion rectangular geometry using a strain of 0.04%. It was found that the wax is a thermo-rheologically simple material that obeys the time-temperature superposition principle. The principle of time-temperature superposition is based on the observation that time and temperature have an equivalent influence on the viscoelastic properties; an increase in temperature corresponds to an extension of the time scale of the experiment. The modulus for thermo-rheologically simple materials is given by:

$$G(t - s, T) = G(\xi(t) - \xi(s), T_0), \quad (\text{Equation 3})$$

where the reduced time, $\xi(t)$, is given as a function of the shift factor, a_T , as:

$$\xi(t) = \int_0^t \frac{1}{a_T(T(\phi))} d\phi. \quad (\text{Equation 4})$$

In addition to the data provided by ARES measurements (Sabau and Viswanathan, 2000), additional measurements were conducted using a bending beam rheometer (BBR). The BBR was introduced as a test method for asphaltic binders (Bahia et al., 1992). Robust procedures have been developed to determine master curves from the bending beam rheometer (Rowe and Sharrock, 2000). The BBR was specifically developed to overcome testing problems that can occur with other methods when testing stiff binders at cold temperatures. The test specimen is a slender beam of wax (125×12.5×6.25 mm) that is simply supported and loaded with a constant force at mid span. The deflection is monitored with time and used for calculation of the stiffness as a function of time (Bahia et al., 1992). The wax was tested with the BBR at temperatures from 0 to 25 °C in 5 °C increments. The optimum fit for the analysis was made with the exclusion of one isotherm from the BBR testing (25 °C) and two isotherms from the torsion bar data obtained with ARES (25 °C and 30 °C).

The shift factor was calculated by a linear regression of the shift amounts used to construct the master curves to the WLF equation (Ferry, 1980):

$$\log_{10}(a_T) = -\frac{C_1(T - T_0)}{C_2 + T - T_0}, \quad (\text{Equation 5})$$

where $T_0=25^\circ\text{C}$, $C_1=-16.21658$, and $C_2=-74.85206$. For a generalized Maxwell-material, the shear relaxation modulus as a function of time, t , is given as:

$$G(t) = g_0 + \sum_{i=1}^N g_i \exp(-t/\lambda_i), \quad (\text{Equation 6})$$

where λ_i are the relaxation times and g_i are the relaxation strengths. These material constants were determined by a nonlinear regression of the master curve data, using the IRIS software (Baumgaertel and Winter, 1989) and are shown in Table 2.

The data presented in this section were measured at temperatures below 55°C where the wax behaves like a hard paste or solid. The wax loses its strength at a temperature just above 60°C. The time-temperature superposition principle may not be applicable across the transition domain when the wax behavior changes from that of a paste to that of a liquid.

BULK MODULUS

For waxes, the constitutive equations for the hydrostatic stress, σ_0 , and dilatation, ϵ_0 , can be simplified by considering that there are no viscous effects in the volumetric deformation. This simplification is widely used for polymeric materials (Bardenhagen et al., 1997; Rezayat and Stafford, 1991; Zoller et al., 1976; and Greiner and Schwarzl, 1984). By taking into account the thermal expansion, the constitutive behavior for the hydrostatic stress and dilatation becomes:

$$\sigma_0 = 3K(\epsilon_0 - 3\epsilon_T), \quad (\text{Equation 7})$$

where K is the bulk elastic modulus. The thermal strain, ϵ_T , can be computed from the density data (Sabau and Viswanathan, 2000).

Table 2: Relaxation times, λ_i , and relaxation strengths, g_i , determined from experimental measurements by nonlinear regression analysis at the reference temperature of 25°C.

No.	g_i (kPa)	λ_i (s)	No.	g_i (kPa)	λ_i (s)
1	8.4000E+04	1.4080E-04	14	4.8090E+03	1.5717E+05
2	5.5456E+04	9.2040E-04	15	3.9863E+03	6.8180E+05
3	5.2022E+04	4.7020E-03	16	4.6647E+03	2.7893E+06
4	4.9323E+04	2.3528E-02	17	3.08056E+03	1.7274E+07
5	4.3975E+04	1.1611E-01	18	2.4393E+03	9.6268E+07
6	3.7048E+04	5.1398E-01	19	2.4446E+03	5.4497E+08
7	3.3772E+04	2.1960E+00	20	1.7370E+03	3.1685E+09
8	3.9505E+04	1.1748E+01	21	1.3903E+03	1.7257E+10
9	2.1745E+04	5.7720E+01	22	9.1295E+02	8.1363E+10
10	1.8180E+04	2.2298E+02	23	6.9663E+02	4.4666E+11
11	1.5983E+04	9.8453E+02	24	6.7480E+02	2.4230E+12
12	1.1557E+04	5.5447E+03	25	2.7218E+03	3.9814E+13
13	8.1935E+03	3.0675E+04			

Data on bulk modulus was obtained from high-pressure dilatometry measurements using a Gnomix PVT apparatus. In high-pressure dilatometry experiments, the change in the volume of a specimen is measured under varying temperatures and pressures. The bulk modulus evaluated at a pressure of 35 MPa and as a function of temperature is shown in Table 3. A detailed discussion on the dilatometry measurements is presented in Sabau and Viswanathan (2000).

Table 3: Bulk modulus evaluated at varying temperatures at a confining pressure of 35 MPa.

Temperature [°C]	K [MPa]	Temperature [°C]	K [MPa]
39	2146.2	80	1460.0
41	1951.7	89	1531.4
51	1482.2	99	1425.6
60	1052.1	109	1452.0
70	1447.8		

WAX PATTERN DIE INSTRUMENTATION

The geometry of the stepped patterns considered for this study is shown in Figure 1. The 2.54 cm thick step is considered to be Step 1. In order to capture the effects of geometrical restraint on the wax pattern dimensions, cores were placed in the die to provide restraint in the pattern.

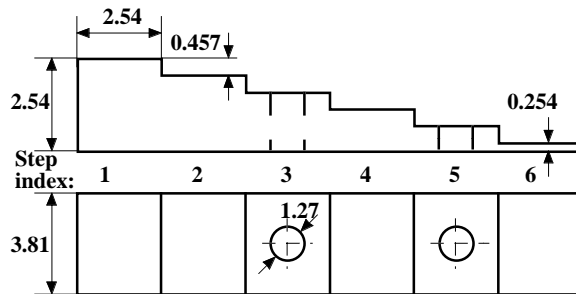


Figure 1: Wax pattern dimensions [cm] and step index.

Several thermocouples were tested for use in this study by dipping them into molten wax (Sabau and Viswanathan, 2001). Inconel sheathed, ungrounded, 0.032 in. diameter thermocouples were chosen for this study, since: (a) the 0.01 in. thermocouples had the best response time but they could not survive the process conditions, (b) they outperformed the similar stainless steel ungrounded thermocouples, (c) they had a response time similar to that of 0.02 in. diameter thermocouples, but were mechanically more robust, and (d) grounded thermocouples picked up ground loops from the wax injection machine and exhibited excessive noise.

The die for the wax pattern had dimensions of 19.5×10.3×9.0 cm. The parting plane of the die almost coincided with the flat surface of the pattern. The centerline of the injection port was in the parting plane of the die. The die was instrumented with thermocouples as shown in Figures 2 and 3. The bottom die (Figure 2) had thermocouples in the wax near the die/wax interface in order to obtain data for estimating the heat transfer coefficient at that interface. The thermocouples in the bottom die were inserted into Steps 1 and 2 of the wax pattern. Thermocouples T1 and T3 were inserted 3.2 mm (0.125 in) into the wax, while thermocouples T2 and T4 were inserted 1.6 mm (0.0625 in) into the wax. Thermocouples were held in place by individual fixtures consisting of a ferule and a 1/8 to 1/16 in pipe thread compression fitting. Thermocouples within each step were placed as close as possible as allowed by their fixtures.

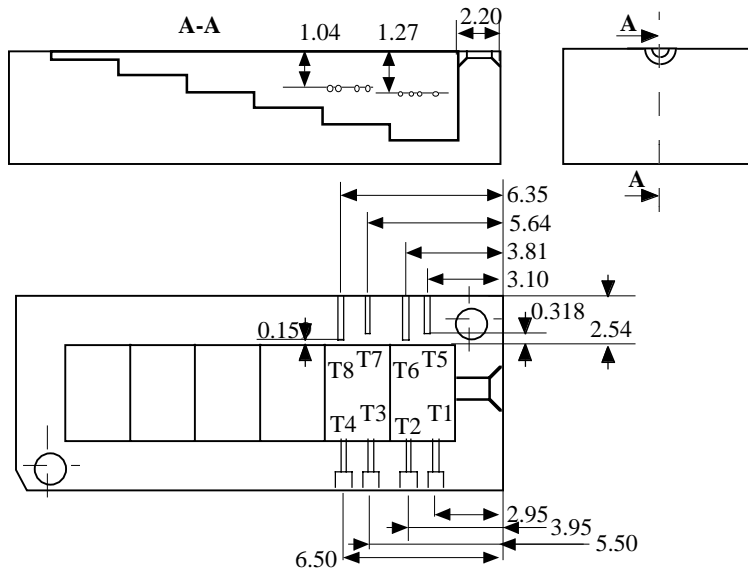


Figure 2. Bottom the die showing thermocouple placement (dimensions in cm). Thermocouple index is also shown.

The top die (Figure 3) contained thermocouples T10-T14 that were inserted into the center of the corresponding steps in the wax pattern. Thermocouple T9 was inserted into the center of the injection port. Pressure transducers (P1 and P2) or thermocouples (T12 and T14) were located at the positions of the core pin inserts, permitting either to be used when core pins were not utilized. The pressure transducers were mounted such that their sensor surfaces coincided with the top (flat) portion of the die cavity.

TEMPERATURE AND PRESSURE MEASUREMENTS

For this work, the wax was injected as a paste using an injection machine that was available at the laboratory facilities of M. Argueso & Co. Due to the configuration of the machine, the die had to be clamped to the machine platen with an external C-clamp. This introduced an extra step in the injection process and also necessitated extra time prior to removal of the wax pattern from the die. The following time intervals are specified during the production of each wax pattern: (a) the dwell time, during which the injection pressure is applied, and (b) the holding period, which is the time elapsed during the removal of the C-clamps. The experimental variables were as follows: injection pressure 2.04 MPa (300 psi), injection temperature 54°C (130°F), dwell time 80 s, and holding time 95 s. An intermediate period of 5 s between the dwell and holding periods, during which the injection pressure is released, was considered in the numerical simulations.

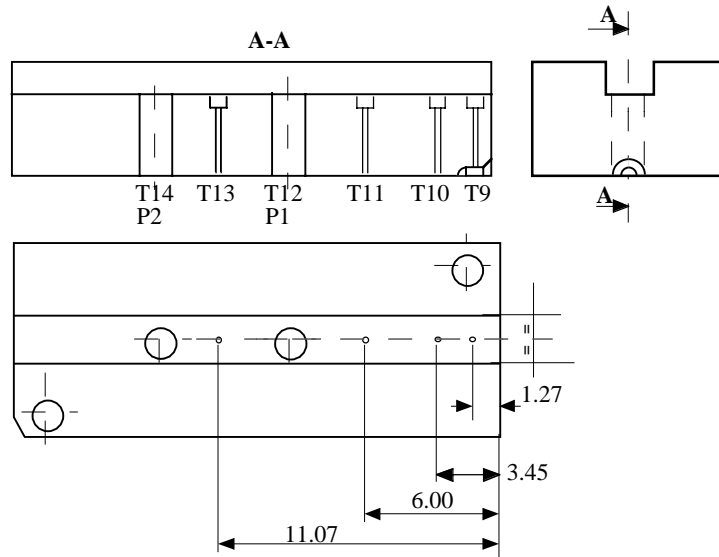


Figure 3. Top die showing thermocouple placement (dimensions in cm). Thermocouple and pressure transducer indices are also shown.

Typical data for the pressure in the wax (transducer P1) and the temperature in the injection port (thermocouple T9) are shown in Figure 4. The instant at which the die was filled with wax is that at which the maximum pressure is recorded (Figure 4). The pressure drops almost linearly throughout the dwell time. The temperature drops steeply in the first 25 s and reaches a plateau at about 90 s. The injection temperature (54°C) is not observed in the cooling curve since the filling time is much smaller than the response time of the thermocouple. About 130 s after the die was filled with wax, pressure ceased to be transmitted into the wax pattern. The instant at which the pressure is not transmitted through the wax pattern is also marked by an inflection in the temperature profile. The data suggests that the wax behaves as a paste until about 29°C. As long as the wax in the injection port is in a paste state, it continues to transmit pressure.

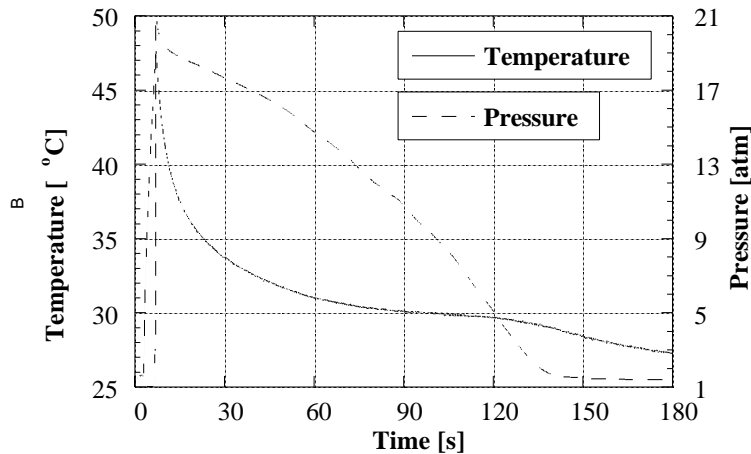


Figure 4: The evolution in time of the temperature in the injection port (thermocouple T9) and the pressure in the wax pattern (pressure transducer P1).

In Figure 5, typical cooling curves in the wax at locations near the wax-die interface are shown for thermocouples T1 to T4, which were placed in Steps 1 and 2 as shown in Figure 2. The die temperature was 28°C (82°F) when the data shown in Figure 5 was collected. The cooling curves for thermocouples T2 and T4 exhibit similar profiles, and exhibit a temperature drop of about 2°C (3.5°F). Thermocouples T1 and T3 exhibit a temperature drop of about 5 and 3.5°C (9 and 6°F), respectively, even though they are at the same distance from the die interface. This is due to the fact that thermocouple T1 is in the corner position, and thus experiences heat losses in two directions, whereas the heat loss at the location of thermocouple T3 is primarily one-dimensional. The data from each set of thermocouples can be used to estimate the heat transfer coefficient at the wax-die interface. Preliminary calculations assuming a linear temperature profile in the wax yielded a heat transfer coefficient at the wax/die interface of 250 W/m²K. However, due to the very low thermal diffusivity

of the wax, the temperature profile near the interface is non-linear, and a more complex heat transfer analysis will be required to obtain more accurate values.

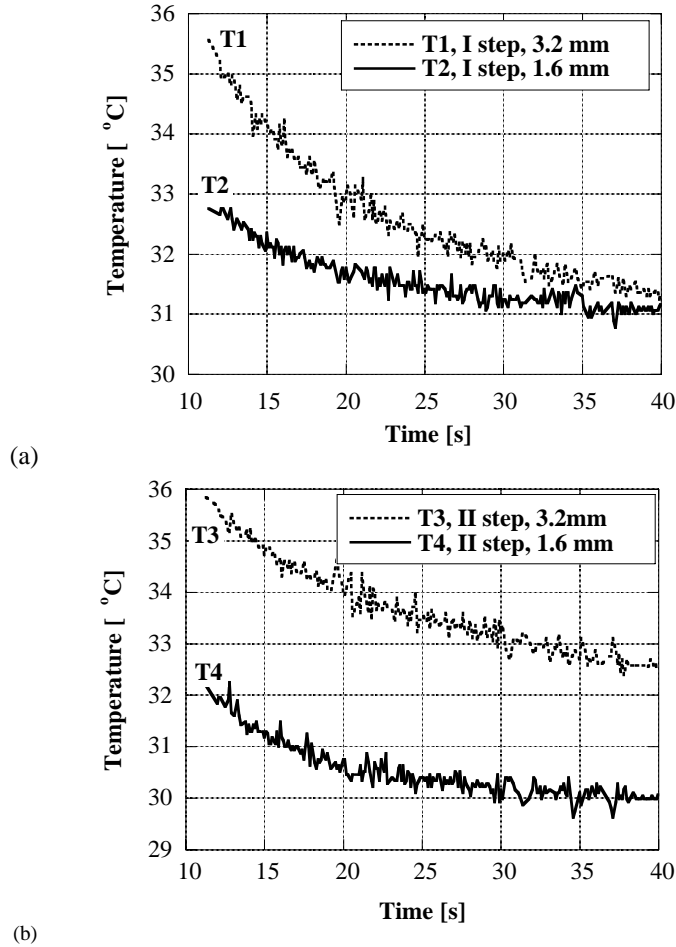


Figure 5: Cooling curves in wax at locations of 3.2 mm (0.125 in.) and 1.6 mm (0.0625 in.) from the wax-die interface for thermocouples (a) T1 and T2 in step 1, and (b) T3 and T4 in step 2.

ANALYSIS OF WAX DEFORMATION

For the problem analyzed in this study, the energy equation was not solved within the die material in order to save computational time. This assumption is based on the fact that preliminary computations indicated that the temperature variation in the die was only about 2°C. An interface heat transfer coefficient of 250 W/m²K between the wax and die was used based on preliminary estimations of experimental data. The temperature of the pattern die was taken to be 28°C. A constant heat transfer coefficient of 4.18 W/m²K was used for the heat transfer coefficient between the wax and the ambient, after the pattern was removed from the die. The ambient temperature was taken to be 22°C. The wax injection phase in which the die is filled with wax was not considered.

Based on the data available for the bulk modulus at a 35MPa confining pressure (Table 3), and the variation of the shear modulus as a function of time (Equation 6 and Table 2), the ratio between the shear modulus and bulk modulus was determined to vary between 0.001 and 0.1. Due to the small ratio between the shear modulus and bulk modulus, the compressibility of the wax was neglected in this study. The elastic modulus was taken to be that of a pure incompressible material, i.e., $E=3G_0$, where $G_0=500$ MPa is the instantaneous shear modulus $G_0 = G(0)$ (Equation 6). A Poisson ratio of 0.48 was used in the numerical simulations since higher Poisson ratios, closer to 0.5, are more difficult to handle in ABAQUS™. A hybrid element, a constant pressure, 8-node thermally coupled brick, with trilinear displacement and temperature, designed for use with incompressible materials, was used in this study. These hybrid elements, in which the pressure is treated as an independent solution variable, are slightly more computationally expensive than traditional elements but more provide better numerical stability in numerical simulations.

The first numerical simulation was performed for the case in which the wax was considered to be a purely elastic material, its viscoelastic behavior was reflected. The second numerical simulation considered the viscoelastic properties of the wax. The comparison between the results of the two numerical simulations will be used to determine the applicability of (a) pure elastic models, which are readily available, and (b) viscoelastic models, which should be more appropriate for wax deformation problems but are not widely available.

The evolution of the temperature field and the ensuing displacements with time were calculated for the cases with and without restraint (i.e., cores). Figure 6 shows the temperature and displacement map for the restrained pattern for the case in which the wax is considered to be a purely elastic material, while Figure 7 shows similar results for the viscoelastic material.

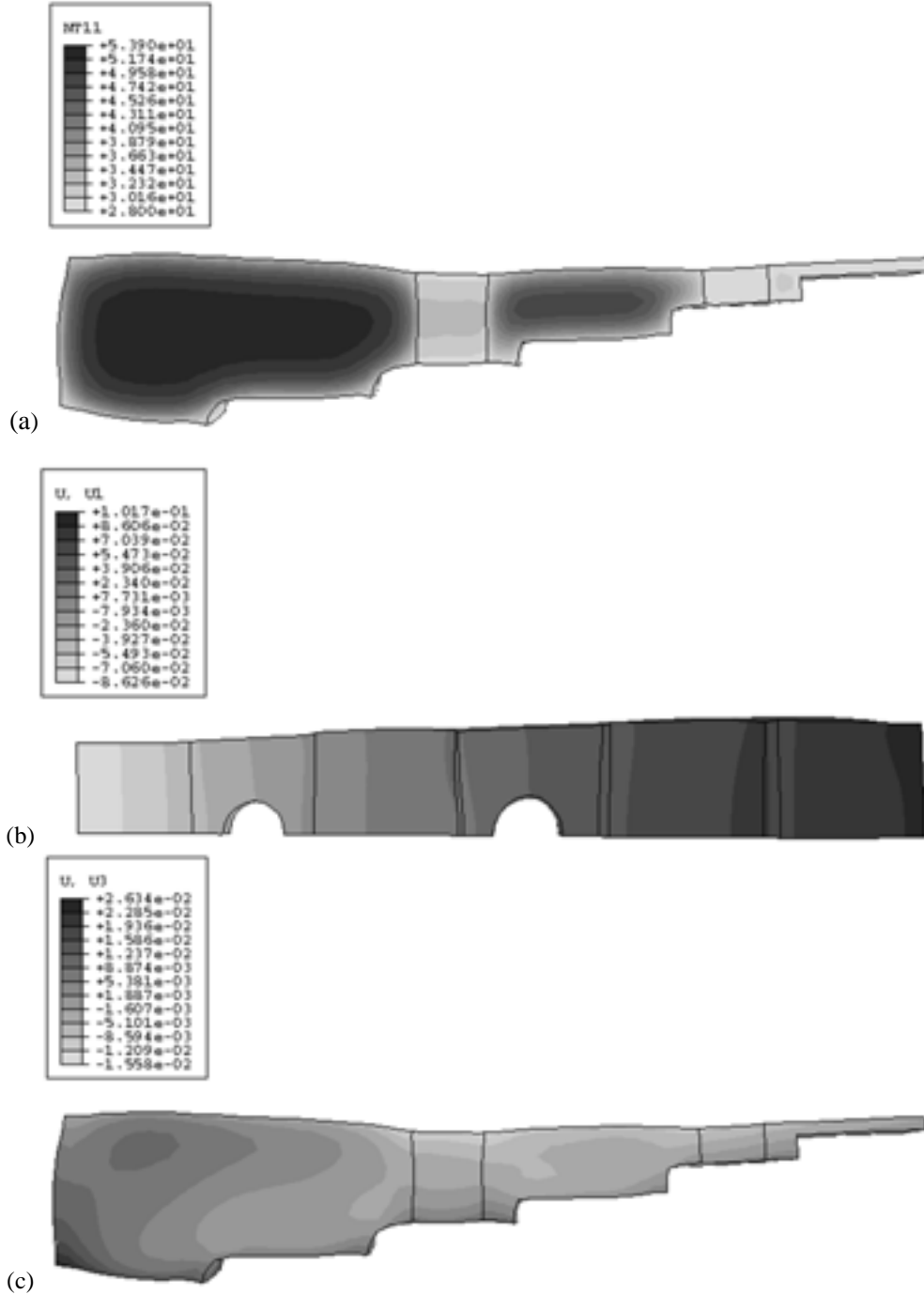


Figure 6: Pure elastic case: (a) Temperature distribution ($^{\circ}\text{C}$), and displacement distribution (cm) right after removal of the wax from the die, (b) vertically along the pattern centerline and (c) horizontally along the pattern thickness. Displacements are magnified 20 times.

The temperature and displacement distributions, which are shown in Figures 6 and 7, were taken at the instant right after the removal of the wax pattern from the die. In Figure 6(a) and 7(a), the temperature distribution is shown for a vertical mid-plane cross section in the wax pattern right before the wax pattern is removed from the die. After cooling in the die for 180 s, a thin layer of solid wax about 2.5 mm thick forms on the surface of the pattern. Due to its low thermal diffusivity, the wax cools very slowly, and most of the wax is still at the injection temperature. The maximum temperature in the wax decreases slowly from an initial value of 54°C to 45, 40, 35, 31, and 26°C approximately 25 min, 50 min, 1.2 h, 1.6 h, and 2.5 h after its removal from the die.

Figures 6(b) and 7(b) show the displacement along the length of the wax pattern. All displacements are relative to the die, and in the x-direction. Negative displacements indicate a contraction towards the injection port. Figures 6(b) and 7(b) indicate that there is significant longitudinal contraction before the pattern is removed from the die.

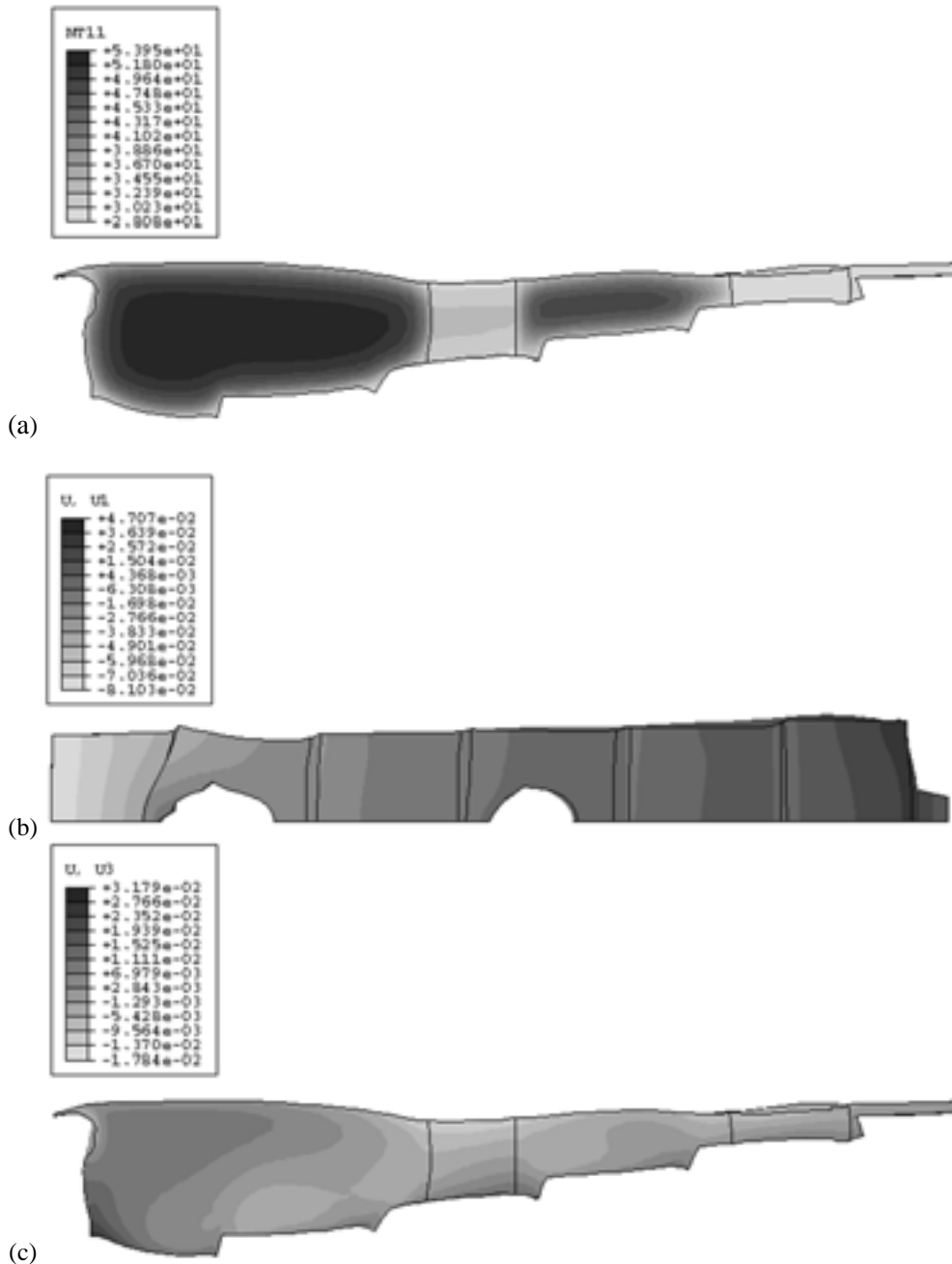


Figure 7: Viscoelastic case: (a) Temperature distribution (°C), and displacement distribution (cm) right after removal of the wax from the die, (b) vertically along the pattern centerline, and (c) horizontally along the pattern thickness. Displacements are magnified 20 times.

After removal from the die, the wax deformation is unconstrained and the initial distortion due to the constraint from the die decreases with time. For the viscoelastic case, the core restraint has a significant effect on wax deformation and the pattern dimensions [Figure 7(b)]. Conversely, core restraint does not have a large effect on the wax deformation in the pure elastic case [Figure 6(b)]. The deformation in the vertical cross-section is similar for both the elastic and viscoelastic models [Figures 6(c) and 7(c)], although the longitudinal contraction is greater for the pure elastic case. The large deformation in the region adjacent to the injection port is only observed with the viscoelastic model.

Figures 8 and 9 show the deformation of the wax pattern at a time of 3.5 h after the pattern has been removed from the die.

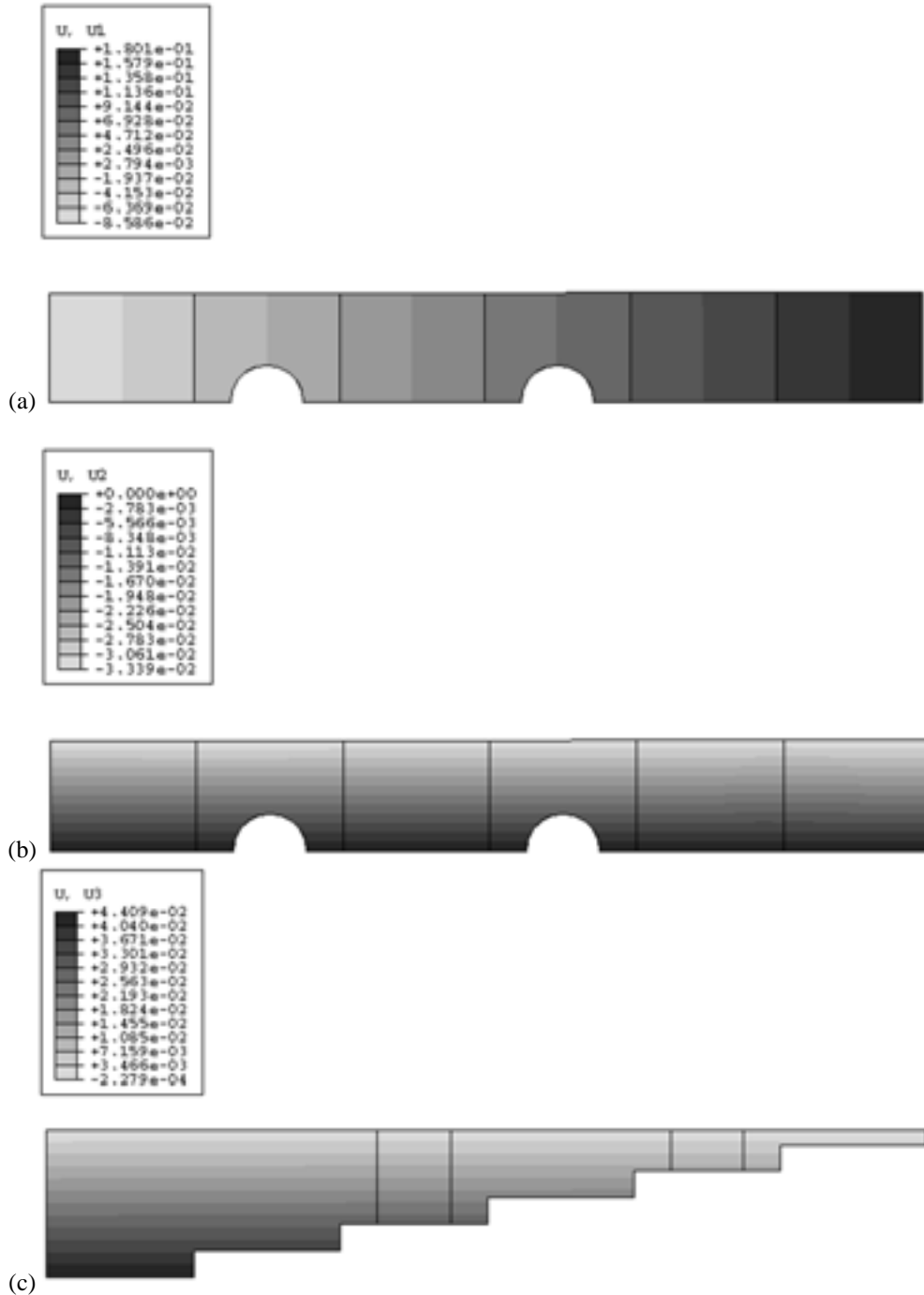


Figure 8: Pure elastic case: Displacement distribution (cm) in the wax pattern, (a) along the pattern length, (b) along the width of the pattern, and (c) along the pattern thickness at 3.5 h after the pattern removed from the die. Displacements are magnified 20 times.

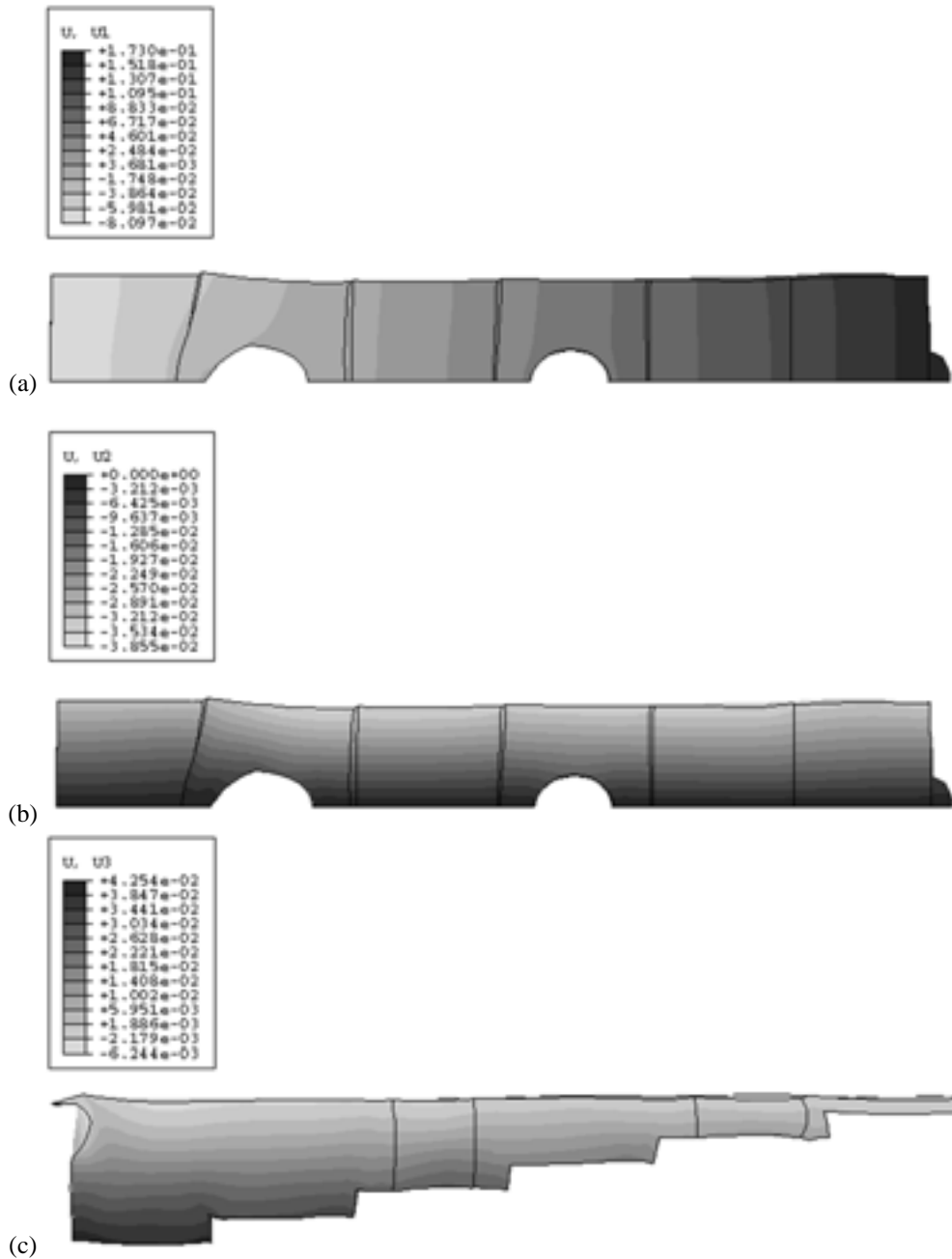


Figure 9: Viscoelastic case: Displacement distribution (cm) in the wax pattern, (a) along the length, (b) along the width, and (c) along the thickness at 3.5 h after the pattern is removed from the die. Displacements are magnified 20 times.

For the pure elastic case (Figure 8), the wax pattern relaxes completely with geometrical features conforming with that of the die, with minimal distortion. In the viscoelastic case, the wax does not relax completely (Figure 8) and residual distortion is evident. The effect of geometric restraint is most evident in step 5, which is only 0.7 cm thick. The distortion is much less significant in step 3, which is also restrained, but is more than twice as thick as step 5. This is supported by industrial experience, i.e., thin sections are more affected by geometric restrictions since they cool faster and relax less than thicker sections as the wax has already hardened while in the die.

Table 4 indicates experimentally measured dimensions of the holes in steps 3 and 5 of the wax pattern. The measurements indicate that the hole in step 5 is more distorted than the hole in step 3. Also, experimental measurements indicate that the holes are elongated in the direction along the plate length rather than normal to the symmetry plane. Experimental measurement of the pattern width also indicates that the width of the pattern decreases in step 5 and that the width of step 4 is

less than that of step 6. The details on wax pattern deformation that have been observed experimentally can also be seen in the numerical simulation results in Figure 9.

Table 4. Experimental and numerical simulation results for hole diameters in step 3 and in step 5.

Dimension*	Diameter for hole in step 3 [mm]			Diameter for hole in step 5 [mm]		
	Measured		Computed	Measured		Computed
	Sample 1	Sample 2		Sample 1	Sample 2	
Dx	12.638	12.592	12.523	12642	12.638	12.678
Dy	12.446	12.432	12.428	12.570	12.508	12.484

*Dx is the hole diameter measured along the length direction.
Dy is the hole diameter measured across the width of the pattern.

The change in pattern length was computed from the displacement data only for the numerical simulation of the viscoelastic case, since the effect of geometric restrained is not captured in the pure elastic model. The evolution of the shrinkage with time is shown in Figure 10. In Figure 10(a) the measured shrinkage is shown, while in Figure 10(b), the numerical simulation results for the shrinkage are shown. The computed shrinkage and the measured shrinkage are 1.09% and 0.26%, respectively, 300 s after removal of the pattern from the die.

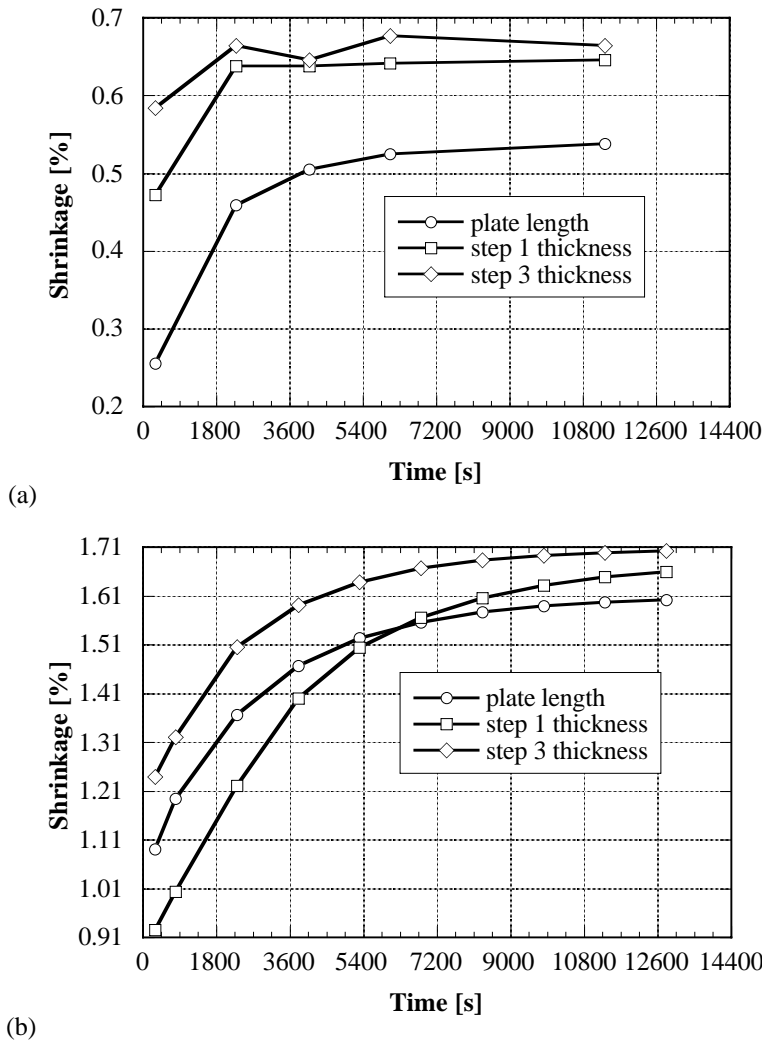


Figure 10: The evolution in time of the linear shrinkage of the wax pattern (a) measured and (b) computed from the viscoelastic data.

The mass of the wax pattern was measured to be 77.18 g. The theoretical mass of the sample at the instant of injection can be computed based on the density of the wax at the injection temperature and the volume of the die cavity. This theoretical mass of the sample was determined to be 73.22 g. The measured mass of the sample is larger than the theoretical mass due to the feeding of wax to compensate for shrinkage during the dwell period when pressure is applied at the injection port. Accordingly, one explanation for the large difference in the computed and measured values is due to the fact that wax feeding during the dwell time was not considered in the numerical simulations. Since the wax is almost incompressible, the wax that is fed into the die during the dwell time must compensate for the shrinkage that takes place when the pattern is in the die.

Differences in the experimental and computational results could also be due to the use a constant value for the heat transfer coefficient at the wax-die interface, and neglecting its variation with the contact pressure or due to the formation of an air gap. Further investigations are underway to (a) account for the effect of wax feeding during the dwell time, (b) determine more appropriate values for the heat transfer coefficient at the wax-die interface, and (c) determine other factors that lead to the overestimation of shrinkage of the wax pattern after removal from the die.

SUMMARY AND CONCLUSIONS

This study is the first attempt to determine wax pattern dimensions using computer models that take into account the thermophysical and rheological behavior of the wax. Cerita 29-51, an industrial unfilled wax, is considered in this study. The wax pattern dimensions are determined using a three-dimensional finite element model for coupled thermal and mechanical analysis developed within the commercial software ABAQUS™. Data considered in the numerical simulations includes thermophysical and thermomechanical properties, restraint of geometrical features by the metal die, and process parameters such as dwell time, platen temperature, injection pressure, and injection temperature.

The results of the numerical simulations indicate that when the pattern wax is in the die, a thin layer of solid wax forms on the surface of the pattern. Due to its low thermal diffusivity, the wax cools very slowly. The viscoelastic model is in qualitative agreement with experimental data. The viscoelastic model accurately captures the distortions in the holes in steps 3 and 5 of the pattern; in particular, both experimental measurements and computations indicate that the holes are elongated along the length rather than along the width, and that the hole in step 5 is more distorted than the hole in step 3. The evolution in time of the shrinkage is similar. However, the total shrinkage is overestimated by a factor of two. The data on the measured and computed mass of wax pattern indicate that wax feeding occurs during the injection phase. The wax that is fed into the die during the dwell time must compensate for the shrinkage that take place when the pattern is in the die. In order to predict wax pattern dimensions accurately, this effect of wax feeding during the dwell time must be considered in computer simulation models.

The experimental and numerical simulation results provide several insights into the wax injection process:

- Pressure is transmitted into the die cavity and the wax continues to flow into the die cavity to feed the shrinkage as long as the wax in the injection port is in a paste state. Wax feeding during the dwell time has a considerable effect on the total shrinkage of the wax pattern.
- Since pressure is not transmitted after the injection port freezes, it should be designed to avoid premature freezing prior to the dwell time.
- Heat transfer models or wax pressure measurements can be used to determine the maximum dwell time, or dimension the injection port such that it does not freeze prematurely.
- Viscoelastic models exhibit good potential for accurately capturing the details of wax pattern deformation. Conversely, pure elastic models are unsuitable for predicting deformation, as any distortion is completely relaxed once the pattern is removed from the die.

ACKNOWLEDGMENTS

This work was performed for the project on Predicting Pattern Tooling and Casting Dimensions for Investment Casting, conducted in collaboration with the 4L Investment Casting Committee of the American Foundrymen's Society and the Cast Metals Coalition. We would like to thank M. Argueso & Co., Inc. for providing the wax for this study, T. Wolf, P. A. Silverstein, W.R. Fricker, and I. Al-Rabadi of M. Argueso & Co., Inc. for assistance with wax injection experiments, G. Rowe of Abatech, Inc. for obtaining the viscoelastic relaxation spectrum from rheometry data, T. A. Parham and C. M. Smith for assistance with pressure transducers thermocouples, G. Romanoski and M. Janney for reviewing the manuscript, and G. Carter for typing the manuscript. The research was sponsored by the U.S. Department of Energy, Assistant Secretary for Energy Efficiency and Renewable Energy, Office of Industrial Technologies, Metal Casting Industries of the Future Program, under contract DE-AC05-00OR22725 with UT-Battelle, LLC.

REFERENCES

- Bahia, H.U., Anderson, D.A., and Christensen, D.W., 1992, "The Bending Beam Rheometer: A Simple Device for Measuring Low Temperature Rheology of Asphalt Binders," *Journal of the Association of Asphalt Paving Technologists*, Vol. 61, pp. 117-153.
- Bardenhagen, S.G., Stout, M.G., and Gray, G.T., 1997, "Three-dimensional, Finite Deformation, Viscoplastic Constitutive Equations for Polymeric Materials," *Mech. of Mat.*, Vol. 25, pp. 235-253.
- BICTA, 1983, "Characterization of Investment Casting Foundry Waxes-Phase 1," Agreement No. 71c/2232: Investment Casting Studies.
- BICTA, 1985, "Characterization of Investment Casting Foundry Waxes-Phase 2," Agreement No. A28B/061: Investment Casting Studies.
- Ferry, J.D., 1980, *Viscoelastic Properties of Polymers*, 3rd Edition, John Wiley and Sons, New York.
- Fielder, H., 1998, "The Relationship between Wax Fillers and Resultant Wax Physical Properties," Paper No. 2, Proceedings of 46th Annual Technical Meeting, Investment Casting Institute, Orlando.
- Greiner, R. and Schwarzl, F.R., 1984, "Thermal Contraction and Volume Relaxation of Amorphous Polymers," *Rheologica Acta*, Vol. 23, pp. 378-395.
- Gustafsson, S.E., 1991, *Rev. Sci. Instrum.* 62(3), pp. 797.
- Himran S, Suwono A, and Mansoori GA, 1994, "Characterization of Alkanes and Paraffin Waxes for Application as Phase-Change Energy-Storage Medium," *Energy Sources*, Vol. 16, pp. 117-128.
- Horacek, M., and Helan, J., 1998, "Dimensional Stability of Investment Casting," Proceedings of 46th Annual Technical Meeting, Investment Casting Institute, Orlando, FL.
- Okhuysen V.F., Padmanabhan, K., and Voigt, R.C., 1998, "Tooling Allowance Practices in the Investment Casting Industry," Paper No. 1, 46th Annual Technical Meeting, Investment Casting Institute.
- Piwonka, T.S., and Wiest, J.M., 1998, "Factors Affecting Investment Casting Pattern Die Dimensions," 1998, *Incast*, Vol. 11, No. 6. pp. 8-13.
- Rezayat M. and Stafford, R.O., 1991, "A Thermoviscoelastic Model for Residual Stress in Injection Molded Thermoplastics," *Polymer Engineering and Science*, Vol. 31, pp. 393-398.
- Rosenthal, H.H., 1979, "Shrink Allowance for Pattern Dies in Investment Casting," Paper No. 2, Proceedings of the 27th Annual Meeting of the Investment Casting Institute.
- Roux, J.H.L., Smith, R.D.F., Turner, R., and Weidema O., 1974, "Fischer-Tropsch Waxes 7. Thermal-Conductivity of Hard Wax," *Journal of Applied Chemistry and Biotechnology*, Vol. 24, pp. 81-91.
- Rowe, G.M., and Sharrock, M.J., 2000, "Development of Standard Techniques for the Calculation of Master Curves for Linear-Visco Elastic Materials," The 1st International Symposium on Binder Rheology and Pavement Performance, The University of Calgary, Alberta, Canada, August 14-15.
- Sabau, A.S., and Viswanathan, S., 2000, "Material Properties for Predicting Wax Pattern Dimensions in Investment Casting," Paper No. 4, 48th Annual Technical Meeting, Investment Casting Institute, Dallas, TX, Oct. 15-18.
- Sabau, A.S., and Viswanathan, S., 2001, "Determining Wax Pattern Dimensions in Investment Casting Using Viscoelastic Models," Paper No. 3, 49th Annual Technical Meeting, Investment Casting Institute, Orlando, FL, Oct. 7-10.
- Zoller, P., Bolli, P., Pahud, V., and Ackermann, H., 1976, "Apparatus for Measuring Pressure-Volume-Temperature Relationships of Polymers to 350°C and 2200 kg/cm²," *Review of Scientific Instruments*, Vol. 47, pp. 948-952.
- Greiner, R. and Schwarzl, F.R., 1984, *Rheologica Acta*, Vol. 23, pp. 378-3 pp. 81-91.